

Supplementary Information

Fe³⁺ and H₂O₂ assisted dopamine rapid polymerization on melamine foam to activate
PMS for organic pollutants degradation

Haoxiang Yan^a, Jianzheng Zhen^{a*}, Yuyuan Yao^{a*}

^aNational Engineering Lab of Textile Fiber Materials & Processing Technology
(Zhejiang), Zhejiang Sci-Tech University, Hangzhou 310018, China

*Corresponding Authors: J. Zhen (E-mail: zhenfangxu2018@163.com), Y. Yao (E-mail: yyy0571@126.com).

Text S1. Characterization methods

The microstructures of MF@Fe@PDA and MF@PDA were assessed by scanning electron microscopy (SEM, Vltra55, Carl Zeiss Corporation, Germany) and the instrument was equipped with an energy dispersive spectroscopy (EDS) system to conduct elemental mapping of the catalysts surfaces. Fourier transform infrared (FTIR) spectroscopy (Nicolet IS 10, Nicolet Corporation, America) was used to detect the chemical bonds in MF@Fe@PDA and MF@PDA. The composition and chemical state of elements before and after the reaction were determined by X-ray photoelectron spectroscopy (XPS, Thermo K-Alpha, Thermo Corporation, USA) using monochromated Al-K α radiation at 1486.6 eV. The electrochemical measurement was conducted on an electrochemical workstation (CHI 660E, CH Instrument, China). UV spectrophotometer (UV-1800, Unico Shanghai Corporation, China) was used to detect changes in absorbance during the degradation process of pollutants. High performance liquid chromatography (HPLC, Agilent 1200, Agilent Corporation, USA) was used to detect degradation products.

Text S2. HPLC measurement

The quantification of variations in the concentrations of two distinct organic contaminants, pharmaceuticals and phenols, was accomplished utilizing high-performance liquid chromatography (HPLC) technology, outfitted with a C18 separation column (dimensions: 150 \times 4.6 mm, particle size: 5.0 μ m, sourced from Waters). For the analysis of pharmaceuticals, an acetonitrile/water mixture (30:70,

volume ratio) served as the mobile phase, while for phenols, a methanol/water blend (40:60, volume ratio) was employed. Both processes operated at a flow rate of 1.5 mL/min, with detection wavelengths tailored specifically to 265 nm for pharmaceuticals and 278 nm for BPA, respectively.

Text S3. EPR method

To obtain the EPR spectra, a Bruker A300 spectrometer was utilized, incorporating DMPO and TEMP as spin traps for capturing the dynamic oxygen species. The experimental setup commenced by the introduction of a precise amount of catalyst sample and PMS into a 100 mL glass flask filled with either deionized water or methanol solution. At specific time intervals during the reaction, a 1 mL aliquot was extracted and promptly neutralized with specific trapping agents: 20 μL of DMPO was used to sequester $\cdot\text{OH}$ and $\text{SO}_4^{\cdot-}$ radicals in water, while 50 μL of TEMP was employed for capturing $^1\text{O}_2$ in water. In the case of methanol, 20 μL of DMPO was added to trap $\text{O}_2^{\cdot-}$ radicals. This mixture was then loaded into a micropipette, with one end securely sealed with vacuum grease, for subsequent EPR analysis. The spectrometer's parameters were adjusted to: a center field of 3510G, a sweep width of 80 G, a microwave frequency of 9.77 GHz, a modulation frequency of 100 kHz, and a power output of 20.00 mW.

Note S1. Kinetics analysis

Utilizing a pseudo-first-order kinetics model (refer to Eq. S1), the rate of reaction

was determined, and the efficacy of contaminant removal was quantified via Eq. S2:

$$\ln (C_0/C_t) = k_{\text{obs}} \times t \quad (\text{S1})$$

$$\text{removal efficiency} = ((C_0 - C_t)/C_0) \times 100\% \quad (\text{S2})$$

Here, C_0 denotes the initial concentration of contaminants, whereas C_t represents the concentration measured at a specific time t during the catalytic reaction. The apparent reaction constant, k_{obs} , is derived from the slopes of the plot, where $\ln (C_0/C_t)$ is plotted against time.

Note S2. The calculation of turnover frequencies (TOF).

The turnover frequencies (TOF, measured per Fe atom) for the elimination of BPA were determined through the calculation based on the initial degradation rate (Rd) of BPA, where Rd is equal to the observed rate constant (k_{obs}) multiplied by the initial BPA concentration.

$$TOF = \frac{R_d}{C_{Fe}} \quad (\text{S3})$$

Note S3. Preparation of MF@Fe@PDA-PH

A solution containing 0.2 g of PH and 10 μl of 38% HCl was dissolved in 10 ml of ethanol. Subsequently, 5 mg of MF@Fe@PDA were introduced into this solution. Following agitation for a period of 24 hours, the resulting precipitate was isolated and subjected to multiple ethanol washes to eliminate any residual PH molecules. After being dried at 60 degrees Celsius for 12 hours, the MF@Fe@PDA-PH sample was successfully obtained.

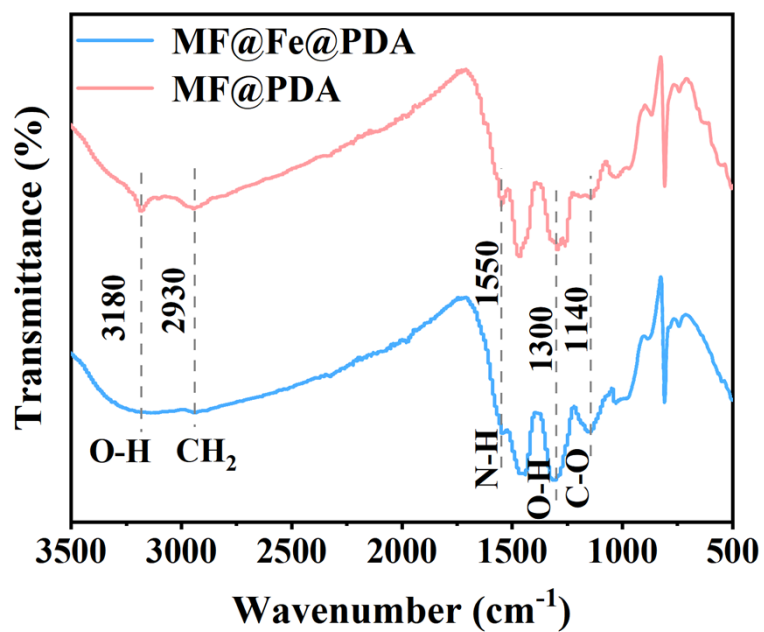


Fig. S1. FTIR spectra of MF@Fe@PDA and MF@PDA.

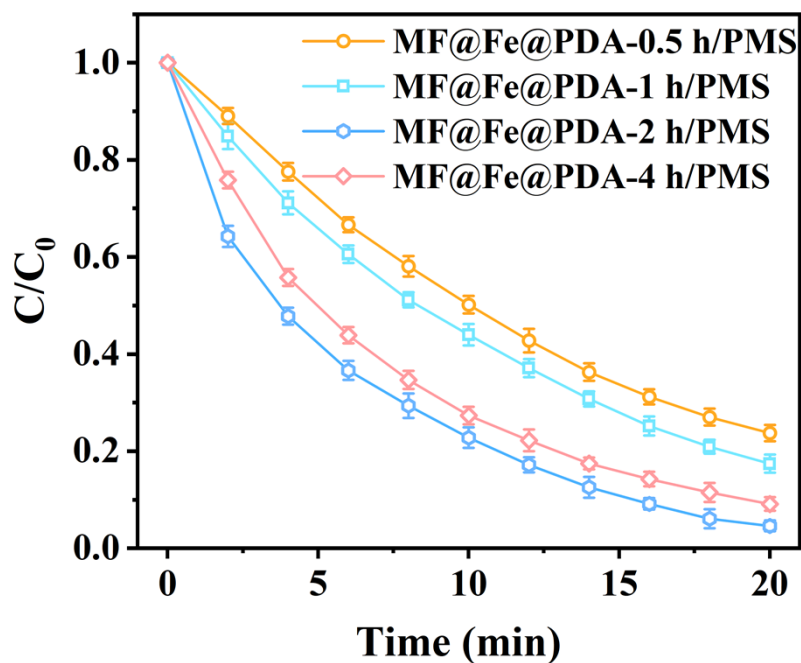


Fig. S2. The effect of dopamine deposition time on the removal efficiency of BPA.

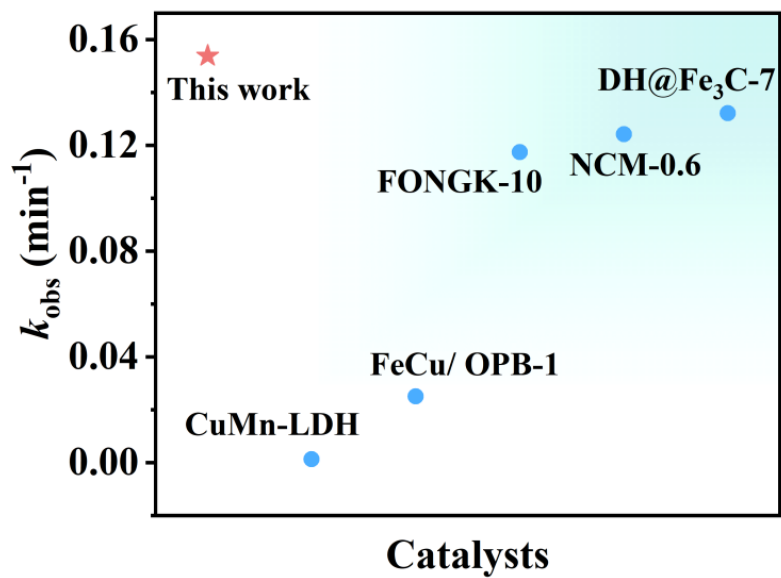


Fig. S3. Comparison of k_{obs} value for BPA degradation in related work.

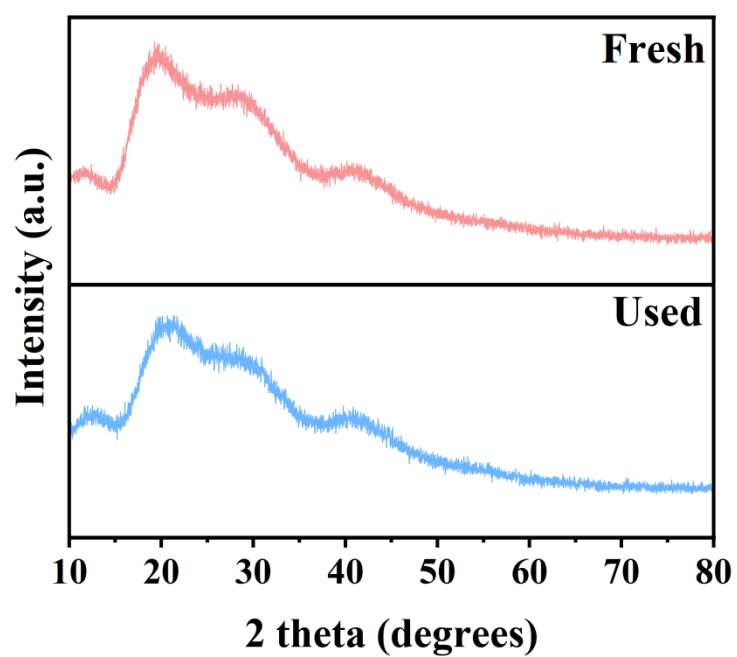


Fig. S4. XRD spectra of the fresh and used MF@Fe@PDA.

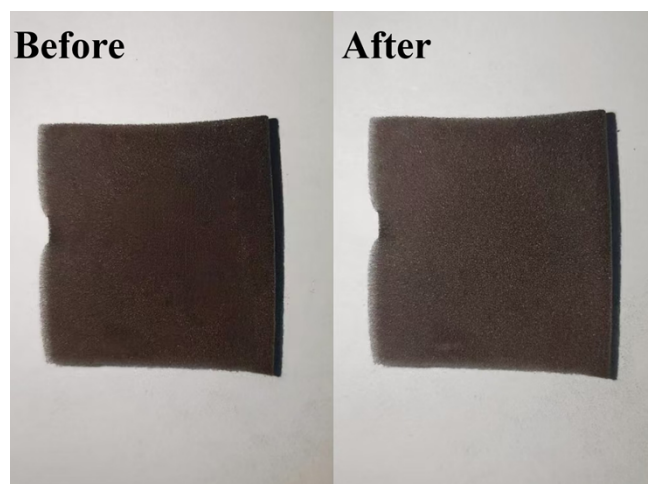


Fig. S5. The physical performance of MF@Fe@PDA before and after reaction.

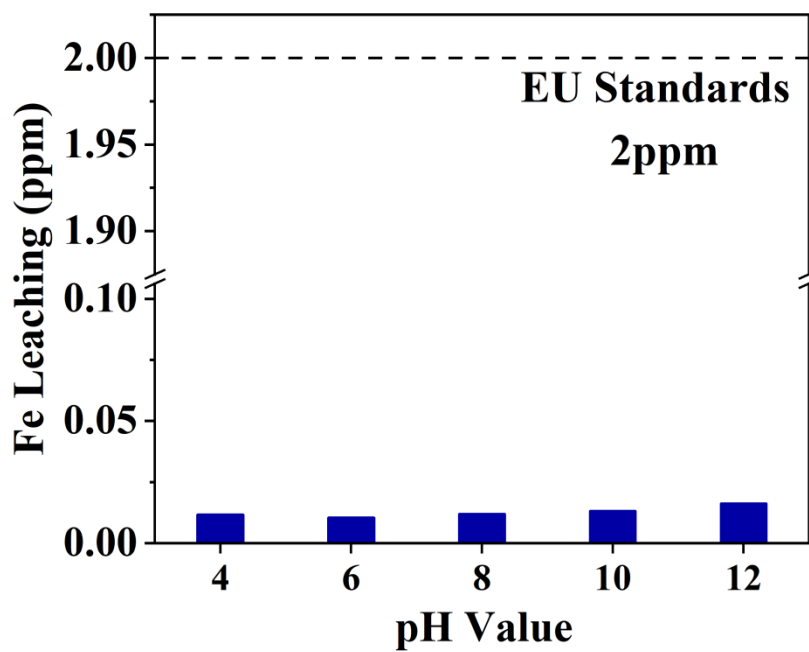


Fig. S6. The leaching amount of Fe in the solution after MF@Fe@PDA degradation of BPA under different initial pH conditions. Conditions: [BPA] = 10 μ M, [PMS] = 0.25 mM, [catalyst] = 250 mg/L, T = 298 K.

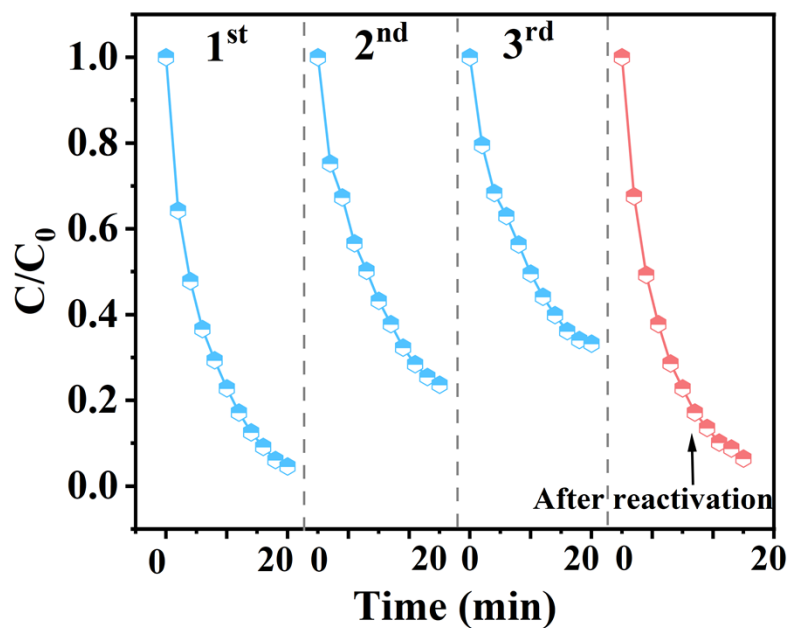


Fig. S7. Cyclic and reactivated degradation of BPA by MF@Fe@PDA/PMS system.

Conditions: [BPA] = 10 μ M, [PMS] = 0.25 mM, [catalyst] = 250 mg/L, initial pH = 5.8, T = 298 K.

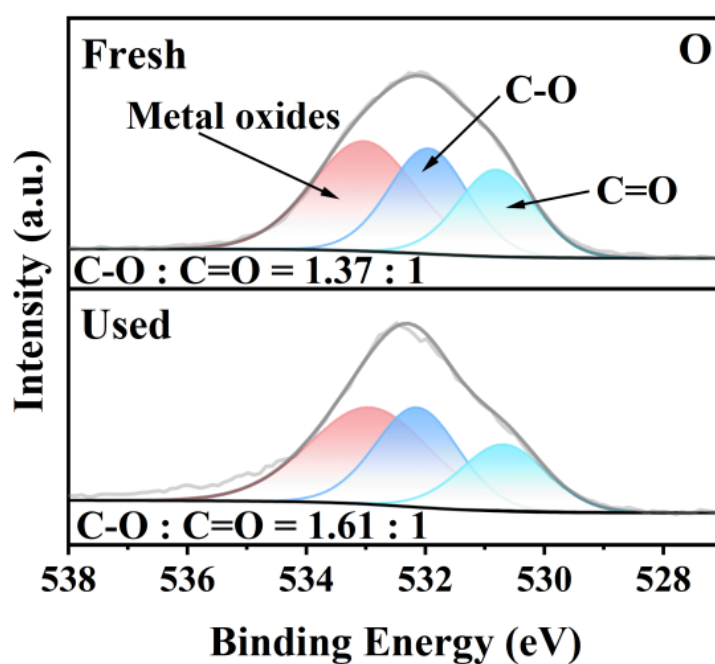


Fig. S8. C 1s XPS spectrum of the fresh and used MF@Fe@PDA.

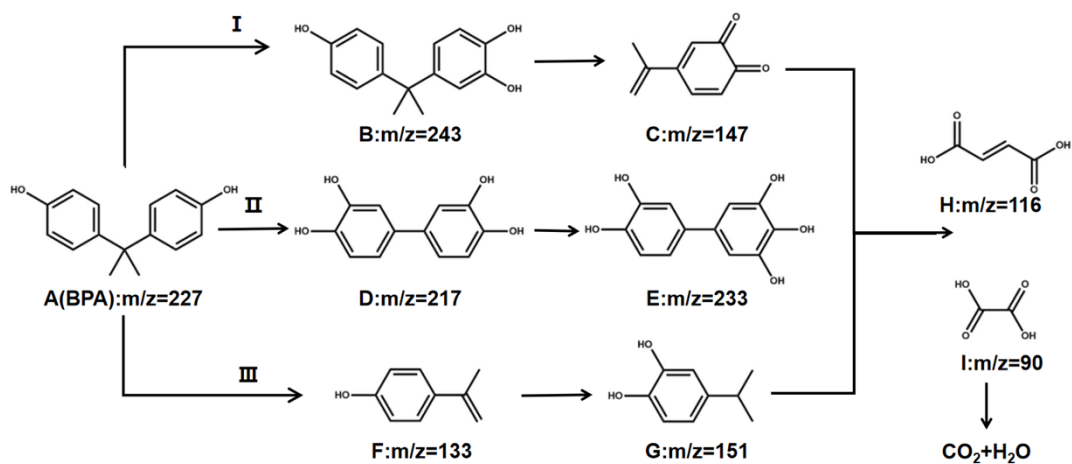


Fig. S9. Possible BPA degradation pathways in MF@Fe@PDA/PMS system.

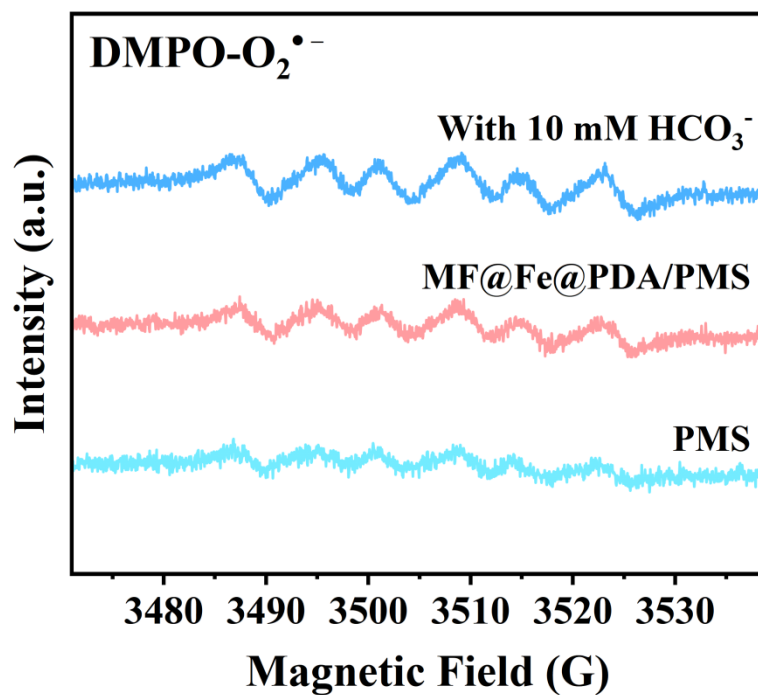


Fig. S10. Spin-trapping EPR spectra of $\text{DMPO-O}_2^{\bullet-}$ adducts in the different systems.

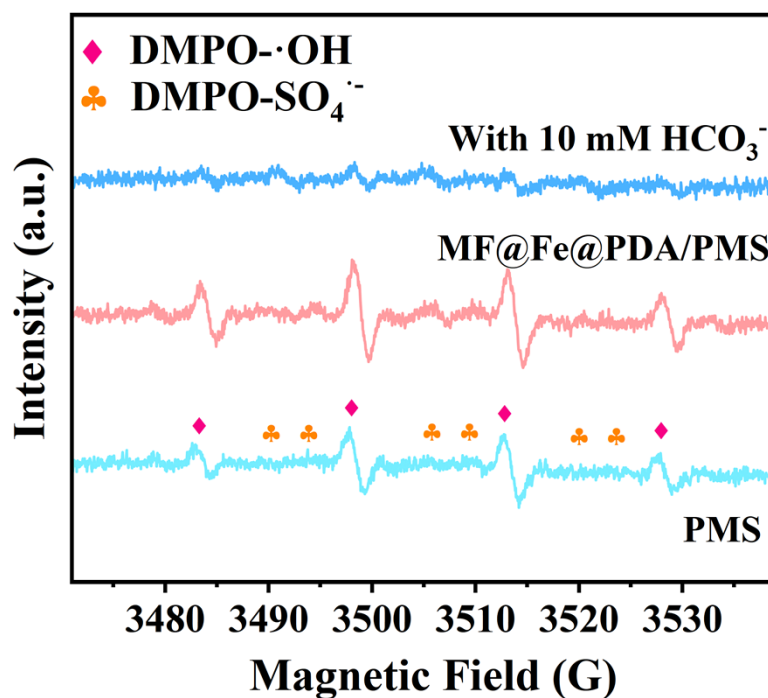
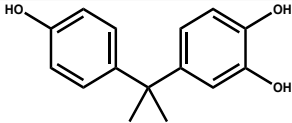
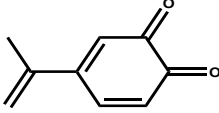
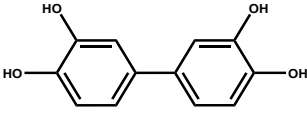
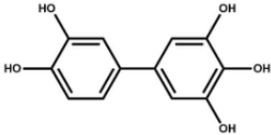
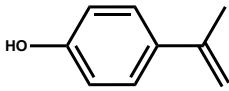
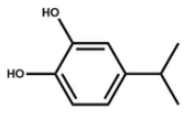
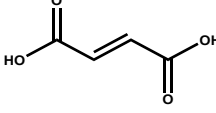
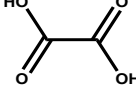


Fig. S11. Spin-trapping EPR spectra of DMPO- \cdot OH and DMPO-SO $_4^{\cdot-}$ adducts in the different systems.

Table S1. Comparison of MF@Fe@PDA and similar catalysts previously reported.

Catalyst	PMS	BPA	Time (min)	Remove rate (%)	k_{obs} values (min $^{-1}$)	Ref.
	concentration (mM)	concentration (μ M)				
MF@Fe@PDA	0.25	10	20	95.39	0.1538	This work
CuMn-LDH	0.92	17.5	40	95	0.00128	24
FeCu/OPB	0.37	87.6	90	90	0.025	25
FONGK-10	0.5	43.8	40	97	0.1174	26
NCM-0.6	0.15	87.6	20	92	0.1242	27
DH@Fe $_3$ C-7	0.75	87.6	40	99	0.1322	28

Table S2. Degradation byproducts of BPA detected by UPLC-MS.

Compound NO.	chemical formula	Molecular structure	MW ^c
B	C ₁₅ H ₁₆ O ₃		243
C	C ₉ H ₈ O ₂		147
D	C ₁₂ H ₁₀ O ₄		217
E	C ₁₂ H ₁₀ O ₆		233
F	C ₉ H ₁₀ O		133
G	C ₉ H ₁₂ O ₂		151
H	C ₄ H ₄ O ₄		116
I	C ₂ H ₂ O ₄		90